Chalmers Publication Library

Copyright Notice

(Article begins on next page)

Phase and amplitude characteristics of a phase-sensitive amplifier operating in gain saturation

Carl Lundström, * **Bill Corcoran, Magnus Karlsson, and Peter A. Andrekson**

Photonics Laboratory, Department of Microtechnology and Nanoscience, Chalmers University of Technology, S-412 96, Göteborg, Sweden

*[*carl.lundstrom@chalmers.se](mailto:carl.lundstrom@chalmers.se)*

Abstract: We investigate a non-degenerate phase-sensitive amplifier (PSA) operating in gain saturation experimentally and numerically using the three-wave model. The phase-dependent gain and phase-to-phase transfer functions are obtained for different levels of saturation with good agreement between experimental and numerical data when higher-order FWM is small. Moreover, we identify an operating point where the PSA is found to be able to significantly reduce both phase- and amplitude noise simultaneously.

© 2012 Optical Society of America

References and links

1. C. M Caves, "Quantum limits on noise in linear amplifiers," Phys. Rev. D **26,** 1817–1839 (1982).
2. Z. Tong, C. Lundström, P. A. Andrekson, C. J. McKinstrie, M. Karlsson, D. J. Blessing, E. Tipsuwannakul, B. J. Puttnam, H. Toda, and L. Grüner-Nielsen, "Towards ultrasensitive optical links enabled by low-noise phase-sensitive amplifiers," Nat. Photonics **5,** 430–436 (2011).
3. K. Croussore and G. Li, "Phase and amplitude regeneration of differential phase-shift keyed signals using phase-sensitive amplification," J. Sel. Top. Quantum Electron. **14,** 648–658 (2008).
4. R. Slavík, F. Parmigiani, J. Kakande, C. Lundström, M. Sjödin, P. A. Andrekson, R. Weerasuriya, S. Sygletos, A. D. Ellis, L. Grüner-Nielsen, D. Jakobsen, S. Herstrøm, R. Phelan, J. O'Gorman, A. Bogris, D. Syvridis, S. Dasgupta, P. Petropoulos, and D. J. Richardson, "All-optical phase and amplitude regenerator for next-generation telecommunication systems," Nat. Photonics **4,** 690–695 (2010).
5. R. D. Li, P. Kumar, and W. L Kath, "Dispersion compensation with phase-sensitive optical amplifiers," J. Lightwave Technol. **12,** 541–549 (1994).
6. C. Lundström, B. Corcoran, S. L. I Olsson, Z. Tong, M. Karlsson, and P. A. Andrekson, "Short-pulse amplification in a phase-sensitive amplifier," in *Optical Fiber Communication Conference*, OSA Technical Digest (Optical Society of America, 2012), paper OTh1C.1.
7. K. Croussore, I. Kim, C. Kim, Y. Han, and G. Li, "Phase-and-amplitude regeneration of differential phase-shift keyed signals using a phase-sensitive amplifier," Opt. Express **14,** 2085–2094 (2006).
8. A. Bogris and D. Syvridis, "RZ-DPSK signal regeneration based on dual-pump phase-sensitive amplification in fibers," IEEE Photon. Technol. Lett. **18,** 2144–2146 (2006).
9. K. Inoue, "Optical level equalization based on gain saturation in fibre optical parametric amplifier," Electron. Lett. **36,** 1016–1017 (2000).
10. Y. Su, L. Wang, A. Agrawal, and P. Kumar, "All-optical limiter using gain flattened fibre parametric amplifier," Electron. Lett. **36,** 1103–1105 (2000).
11. M. Matsumoto, "Regeneration of RZ-DPSK signals by fiber-based all- optical regenerators," IEEE Photon. Technol. Lett. **17,** 1055-1057 (2005).
12. M. Sköld, J. Yang, H. Sunnerud, M. Karlsson, S. Oda, and P. A. Andrekson, "Constellation diagram analysis of DPSK signal regeneration in a saturated parametric amplifier," Opt. Express **16,** 5974–5982 (2008).
13. C. Lundström, Z. Tong, M. Karlsson, and P. A. Andrekson, "Phase-to-phase and phase-to-amplitude transfer characteristics of a nondegenerate-idler phase-sensitive amplifier," Opt. Lett. **36,** 4356–4358 (2011).

14. C. Lundström, B. Corcoran, Z. Tong, M. Karlsson, and P. A. Andrekson, "Phase and amplitude transfer functions of a saturated phase-sensitive parametric amplifier," in *37th European Conference and Exposition on Optical Communications*, OSA Technical Digest (CD) (Optical Society of America, 2011), paper Th.11.LeCervin.4.

15. G. Cappellini and S. Trillo, "Third-order three-wave mixing in single-mode fibers: exact solutions and spatial instability effects," J. Opt. Soc. Am. B **8,** 824–838 (1991).

16. Z. Tong, A. Bogris, M. Karlsson, and P. A. Andrekson, "Full characterization of the signal and idler noise figure spectra in single-pumped fiber optical parametric amplifiers," Opt. Express **18,** 2884–2893 (2010).

17. R. Slavík, J. Kakande, F. Parmigiani, L. Grüner-Nielsen, D. Jakobsen, S. Herstrøm, P. Petropoulos, and D. J. Richardson, "All-optical phase-regenerative multicasting of 40 Gbit/s DPSK signal in a degenerate phase sensitive amplifiers," in *Proceedings European Conference on Optical Communications 2010*, paper Mo.1.A.2.

1. Introduction

Phase-sensitive amplifiers (PSAs) based on fiber four-wave mixing (FWM) (phase-sensitive parametric amplifiers) have recently attracted significant experimental attention. They amplify only one quadrature of the signal light, while attenuating the other, which leads to several intriguing properties. In addition to the possibility of noiseless amplification [1, 2], a PSA can perform phase squeezing of the signal field, in principle providing a signal output in only a single quadrature. This unique capability can be exploited in different signal processing applications, such as phase regeneration of binary phase shift keying (BPSK) signals [3,4] and pulse compression [5,6].

The PSA will convert any phase noise (PN) to amplitude noise (AN) since its gain is phase-dependent with an ultrafast (fs-scale) time response. In [4], Slavík et. al. achieved very good performance by operating the PSA in gain saturation in order to both reduce the inherent PN to AN conversion as well as to suppress any existing amplitude noise on the input signal by amplitude limiting, as had previously been suggested in e.g. [7, 8]. AN-reduction using the amplitude-limiting property of a saturated phase-insensitive parametric amplifier has been investigated for both amplitude [9, 10] and phase-encoded signals [11, 12]

In regenerating the optical phase using PSAs it is therefore desired to operate the PSA in saturation. To enable this, the PSA must be saturated over the entire range of phases for which one wishes to squeeze both PN and AN. Since the PSA small-signal gain can vary significantly with modest changes in phase, this can mean that a very high level of saturation is needed. However, a large saturation also means a reduction in the FWM efficiency and thus, in the efficiency of the phase squeezing. Hence, this raises the question of what level of saturation is optimal, and how the phase-to-phase transfer function is modified as the amplifier is saturated.

We have previously analytically and experimentally investigated the phase-to-phase and phase-to-amplitude transfer characteristics of a non-degenerate-idler PSA in the small-signal regime [13]. Here, we extend this investigation to also include the case of pump depletion. Preliminary experimental work was presented in [14], which we expand upon and support with numerical data. The numerical results are obtained using the three-wave model which is well known [15]. It is important to note that while our investigation concerns the non-degenerate-idler scheme (signal and idler are two discrete waves both carrying the same information positioned in frequency symmetrically around the pump) the results can qualitatively be extended to the degenerate-idler case (signal and idler are degenerate and positioned in frequency in between two pump waves). In one case, the pump pair is degenerate, in the other the signal-idler pair is degenerate, but the qualitative behavior of the phase-dependent gain and phase squeezing are similar. We choose to work with the non-degenerate idler-configuration, as it allows different phase-matching to be easily achievable, and also because quick switching between phase-insensitive (PI) and phase-sensitive (PS) operation is possible in experiments, simply by blocking the idler.

An important consideration is higher-order FWM processes that is not accounted for in the

three-wave model. If the signal/idler powers are large, such higher-order processes may be unavoidable in practice and degrade the efficiency of the first-order process and thus the regeneration properties as well. However, we choose the three-wave model since it is well understood, and also because it is instructive to isolate the first-order process to understand the fundamental trade-offs between amplitude- and phase compression that we describe here.

2. Three-wave model results - transfer functions

To study the effect of pump depletion on the phase response of a phase-sensitive fiber optical parametric amplifier we numerically solve the system of coupled equations (1)-(3):

$$i\frac{dA_p}{dz} = \gamma \left[|A_p|^2 + 2|A_s|^2 + |A_i|^2 \right] A_p + 2\gamma A_s A_i A_p^* \exp\left(-i\Delta kz\right) \tag{1}$$

$$i\frac{dA_s}{dz} = \gamma \left[2|A_p|^2 + |A_s|^2 + 2|A_i|^2 \right] A_s + \gamma A_i^* A_p^2 \exp\left(i\Delta kz\right) \tag{2}$$

$$i\frac{dA_i}{dz} = \gamma \left[2|A_p|^2 + 2|A_s|^2 + |A_i|^2 \right] A_i + \gamma A_s^* A_p^2 \exp\left(i\Delta kz\right), \tag{3}$$

where A is the complex amplitude, subscripts p, s and i denote pump, signal and idler respectively, $*$ represent the conjugation operation, γ is the nonlinearity coefficient, Δk is the low-power propagation constant mismatch and z is the length coordinate in the propagation direction of the fiber.

By varying the input phase of the signal and idler simultaneously, the phase-to-phase and phase-to-amplitude transfer functions can be obtained. The signal and idler should also be equal in power for maximal efficiency [13].

Figure 1(a)-(b) shows the gain and phase-to-phase transfer function calculated using the three-wave model for an ideally phase-matched PSA ($\Delta k = -2\gamma P_{P0}$, where P_{P0} is the pump power at $z = 0$). It had a γL-product of 2.925 W^{-1} and a pump power of 1.97 W, so that the maximal small-signal PSA gain is 50 dB. The curves are calculated for four different input signal powers, here shown in relation to the input pump power. In the small-signal case, the three-wave-model gives the same result as the simpler model used in [13]. For larger signal powers, the amplitude curves saturate over a larger range of input phases, showing the possibility to efficiently suppress phase-to-amplitude noise conversion. However, the phase-to-phase curves also start to show a non-uniformity, meaning that the phase squeezing is compromised. Essentially, there is a trade-off between amplitude and phase flatness. Nevertheless, very efficient phase compression can still be attained with very low phase-to-amplitude conversion over a wide range of input phases e.g. for an input signal power 48 dB below the input pump power. For excessively large input signal powers, both phase and amplitude curves are distorted. Figure 1(c) shows the corresponding (normalized) trajectories in complex-signal space. (The input signal sweeps all phases uniformly at constant amplitude). For easier visualization, each trajectory is rotated 45 degrees relative to the the preceding trajectory. We see that in complex space, saturation manifests as the signal trajectory assuming a spiraling, S-shaped form, instead of the straight line in the small-signal case.

In Fig. 1(d)-1(f) and 1(g)-1(i), the transfer functions and complex-space trajectories are shown for ideally phase-matched PSAs with the same γL-product as before but pump powers of 0.79 W and 0.40 W, giving small-signal gains of 20 dB and 10 dB, respectively. In (f), each trajectory is rotated 45 degrees relative to the the preceding. As expected, larger small-signal gain means that a smaller signal power relative to the pump power at the input is required to saturate the PSA. Moreover, larger small-signal gain means that the PSA can be saturated over a larger range of input signal phases, since there is a wider range of phases with large enough
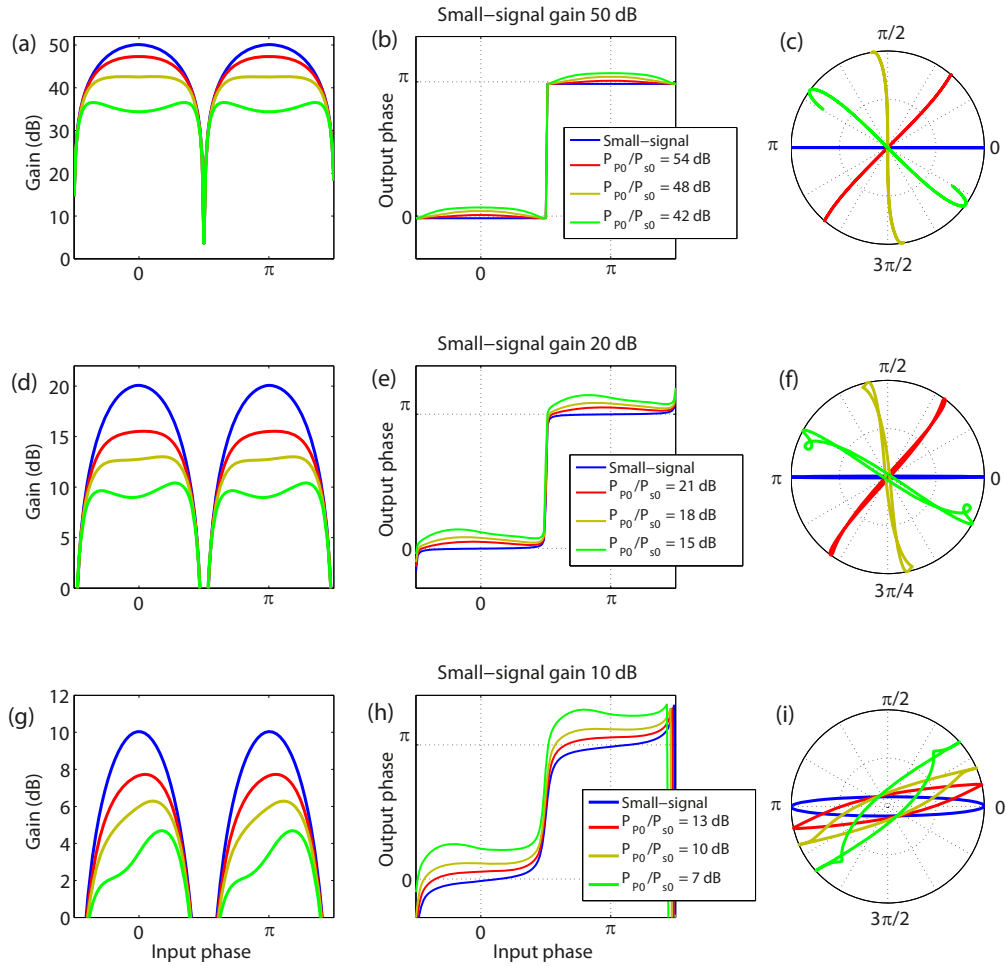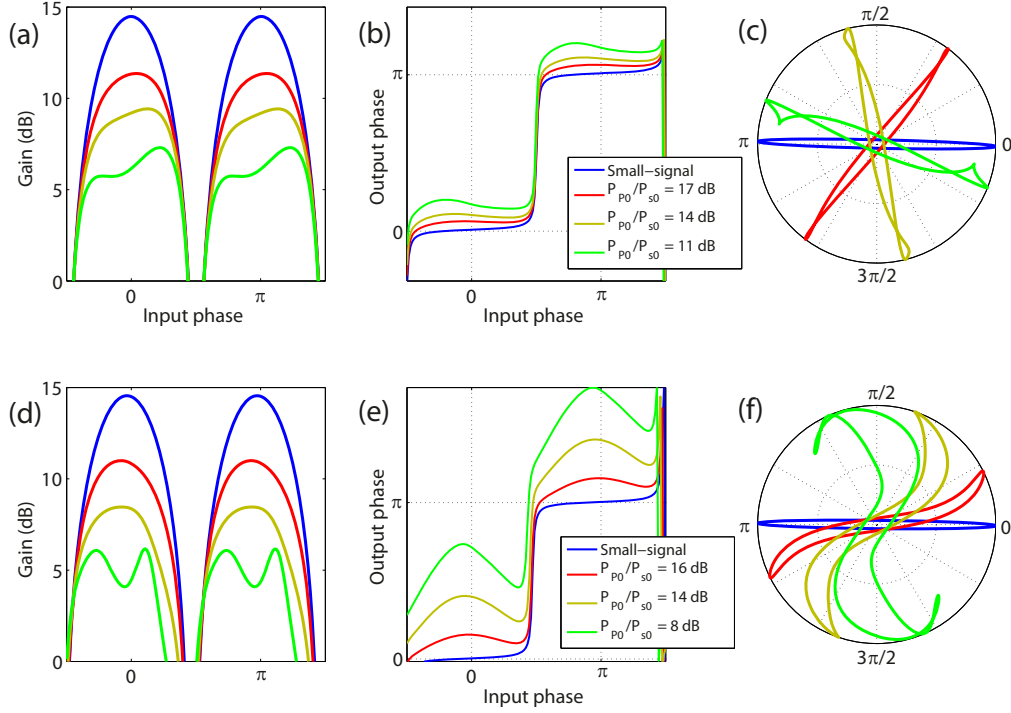
Fig. 1. Calculated phase-dependent gain, phase-to-phase transfer functions and correspond-
ing complex-signal space trajectories for a PSA with $\Delta k = -2\gamma P_{P0}$ (ideally phase-matched)
but different small-signal gains.

small-signal gain to experience sufficient saturation (and indeed a smaller range of phases that is attenuated rather than amplified). When the small-signal gain is only 10 dB (Fig. 1(g)-(i)), however, the gain curve is not flattened very well, but rather takes on a skewed shape. Instead, the phase-to-phase transfer is flattened, e.g. for an input signal power 10 dB below the input pump power, since it is not as flat for lower gains [13]. For large input signal powers, both phase and gain curves are distorted.

Fig. 2. Calculated phase-dependent gain, phase-to-phase transfer functions and corresponding complex-signal space trajectories for a PSA with $\Delta k = -2\gamma P_{P0}$ (top) and $\Delta k = 0$ (bottom) but small-signal gains maintained at 14.5 dB in both cases.

Next, we investigate the impact of the phase-matching. It can be convenient to position the signal/idler frequencies close to that of the pump(s), as in e.g. [4], e.g. in order to fit all waves within the bandwidth of an Erbium-doped fiber amplifier (EDFA) or to avoid unwanted Raman-induced power transfer between waves. However, doing so limits the phase-matching efficiency and thus the gain to be growing only approximately quadratically with the $\gamma P_{P0}L$-product ($\Delta k = 0$), as opposed to exponentially, as in the case of ideal phase-matching ($\Delta k = -2\gamma P_{P0}$).

Figure 2(a)-2(c) and 2(d)-2(f) shows the the transfer functions and complex-space trajectories for different input signal/pump power ratios for PSAs with $\Delta k = -2\gamma P_{P0}$ and $\Delta k = 0$, respectively, but pump power varied to keep the small-signal gain at 14.5 dB in both cases. The γL-product was 2.925 W^{-1} as before, but the pump power was 0.57 W in the exponential gain case and 0.88 W in the quadratic gain case. In Fig. 2(c), each trajectory is rotated 45 degrees relative to the the preceding for easier visualization. In the ideally phase-matched case (Fig. 2(a)-(c)), the distortions of the phase-to-phase transfer function is much smaller. Moreover, a larger range of phases can be saturated in the ideally phase-matched case. In complex-signal space, this is manifested as relatively straight trajectories in the ideally phase-matched case,

with much more pronounced S-shapes in the case of $\Delta k = 0$, showing its much larger variations in output phase. Good phase-matching thus means better regenerator performance, both in amplitude and phase.
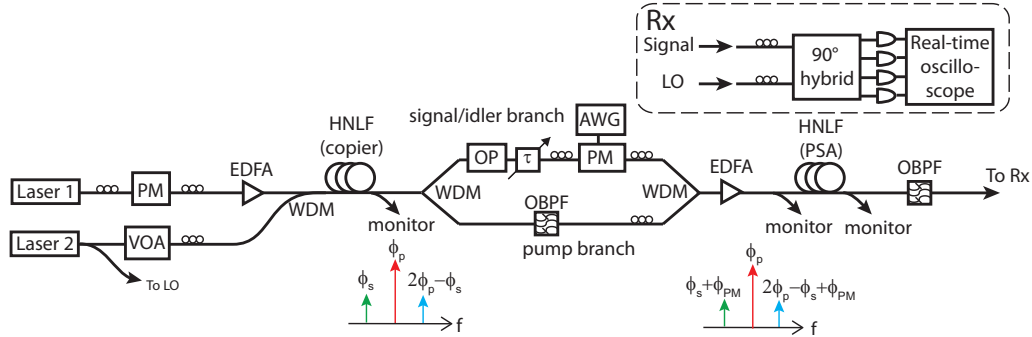
3. Experiment

Fig. 3. Experimental setup. The acronyms are explained in the text.

To verify that the results obtained using the three-wave model are valid also in experimentally realistic conditions we studied the phase-to-phase and phase-to-amplitude transfer functions of a saturated PSA experimentally, under different conditions. The experimental setup is shown in Fig. 3. The copier generated three phase-correlated waves through FWM. A DFB laser at 1554.1 nm and a tunable laser were used as a pump source and signal, respectively. The pump was phase modulated with three RF tones to suppress Stimulated Brillouin Scattering (SBS) prior to amplification by a high-power EDFA. Power from the signal laser was tapped off to be used as the local oscillator (LO) in the receiver. The pump and signal were combined by a WDM coupler that also serves to filter out amplified spontaneous emission (ASE) from the EDFA, and passed into the copier where an idler wave was generated. The copier was implemented in highly nonlinear fiber (HNLF) with length, zero dispersion wavelength (λ_0) and nonlinearity coefficient (γ) of 150 m, 1553.6 nm and 10 (W·km)$^{-1}$, respectively. After the copier, which had a gain of about 10 dB, the pump and signal/idler were separated into separate branches by another WDM coupler. The powers of the signal and idler were controlled by a programmable optical processor (OP). To sweep the input signal and idler phases over all phase states uniformly, a phase modulator driven by a sawtooth wave from an arbitrary waveform generator (AWG) was used. No compensation of slow phase drifts between the arms was needed, since the measurement times were shorter than any such drifts. The pump was then recombined with the signal and idler by another WDM coupler, amplified by an EDFA and finally injected into the PSA, which was implemented with 250 m HNLF with a (λ_0) of 1542 nm and a γ of 11.7 (W·km)$^{-1}$. Polarization controllers were used to ensure that the waves remain aligned in polarization.

The PSA HNLF provided maximum gain at a signal wavelength of 1544.0 nm when pumped with about 0.8 W at 1554.1 nm. Monitor taps was available before and after the PSA. The PSA output signal was filtered and combined with the LO by a 90° optical hybrid. The hybrid outputs, corresponding to the two quadratures of the signal, were detected using balanced detection with a real-time sampling oscilloscope. The measured signal was subsequently filtered in software to remove the distortion at the RF frequencies of the SBS suppression phase modulation.
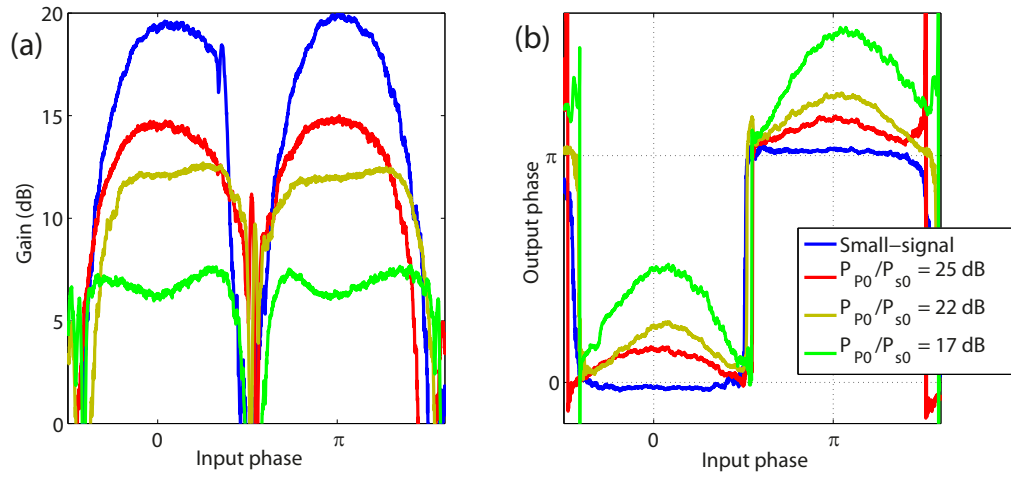
Fig. 4. Experimentally measured phase-dependent gain (a) and phase-to-phase transfer functions (b) for a PSA operating at the peak gain wavelength.
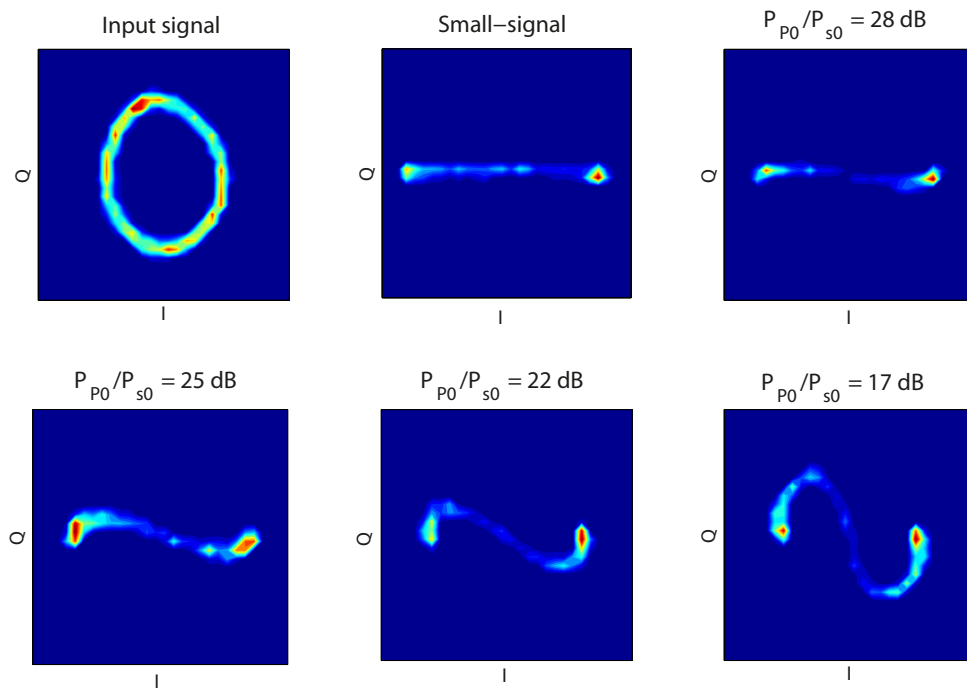

Fig. 5. Experimentally measured complex-space trajectory heat-maps for a PSA operating at the peak gain wavelength.

Figure 4 shows the experimentally measured phase-dependent gain and phase-to-phase transfer function for different input signal powers. The signal wavelength was 1544.0 nm, i.e. at peak (exponential) gain, $\Delta k \approx -2\gamma P_{P0}$, and the pump power into the PSA was kept at about about 0.8 W, giving a maximal PS small-signal on-off gain of about 20 dB. The maximal gain at each input signal level was measured separately using a countinous-wave signal and has an uncertainty of about 1 dB. In the small-signal regime, the phase-to-phase transfer is nearly perfectly flat, with sinusoidally phase-dependent gain. As the signal power is increased the gain curves start to flatten, but the phase-to-phase transfer function becomes somewhat distorted. There is a clear trade-off between flat gain and flat phase-to-phase transfer. At a pump-to-signal power ratio of about 22 dB, the gain curves are nearly flat over approximately ± 1 rad around the two center phases (defined as 0 and π rad). At the same time, however, the phase-to-phase transfer has lost its flatness and varies about 0.8 rad as the input phase varies π rad. In the complex plane, shown as heat-maps in Fig. 5, this manifests as an S-shaped trajectory, as opposed to the real-axis-only straight line in the small-signal regime, and constant-amplitude circle at the PSA input. As the saturation becomes even deeper, the curves are further distorted, with even larger output phase variations and a dip in the gain curves for the phases where the small-signal gain is largest, which corresponds to a larger spiral in the complex plane.

The agreement between measured results and the numerical results from the three-wave model presented in Fig. 1 is very good. In the experimental case, slightly lower input signal powers than in the numerical results were required to achieve the same levels of saturation, which is believed to be due to additional depletion of the pump by higher-order FWM and/or Raman-induced power transfer.
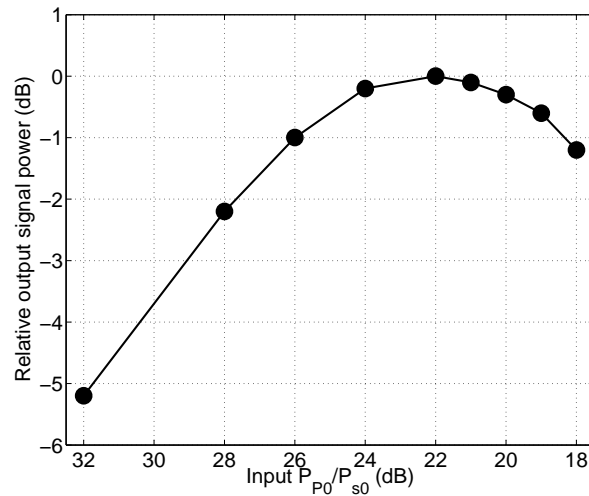

Fig. 6. Measured relative output signal power versus input pump-to-signal power ratio at the phase giving maximal gain for a PSA operating at the peak gain wavelength.

In Fig. 6 the measured maximum output signal power versus input pump-to-signal power ratio (the pump remained constant in power) is shown in the peak gain-case. It can be observed that the pump-to-signal power ratio found to give the flattest phase-dependent gain (22 dB) is also the ratio giving the largest absolute output power, which also is where the signal power response is at its flattest.

Figure 7 shows the measured phase-dependent gain and phase-to-phase transfer functions of the PSA for different input signal powers, when $\Delta k \approx 0$ (quadratic gain). The signal wavelength
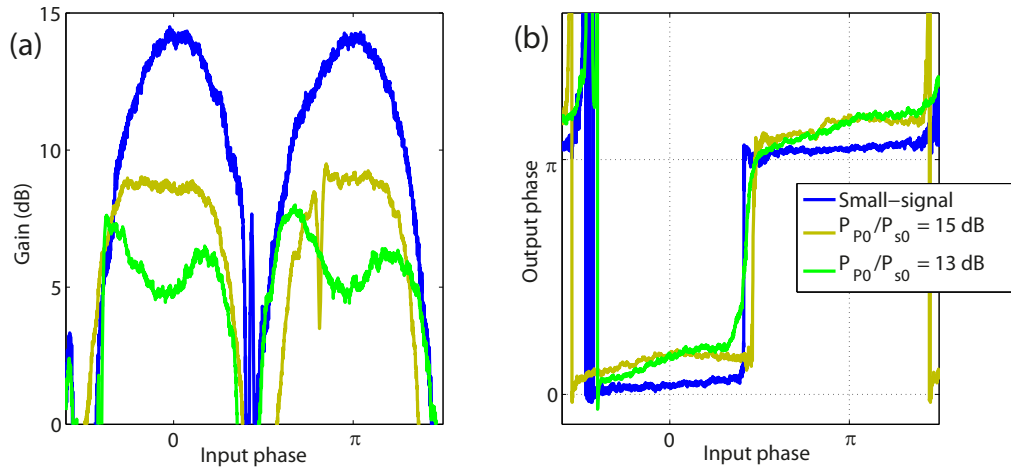
Fig. 7. Experimentally measured phase-dependent gain (a) and phase-to-phase transfer functions (b) for a PSA operating in the quadratic gain regime with a pump-to-signal wavelength spacing of 2.1 nm.

was 1552.0 nm and the pump power into the PSA remained the same as above at about 0.8 W, giving a maximal PS small-signal gain of about 14.5 dB. Even in the small-signal case, one can see that there is a small tilt in the phase-to-phase transfer curve which is what one expects for lower-efficiency (lower gain) PSA [13]. For approximately 15 dB pump-to-signal power ratio, the gain curves are reasonably flat over ± 0.5 rad around the two center phases, with a moderate variation of around 0.5 rad in the output phase when the input phase varies π rad. With even larger input signal power, the efficiency is further reduced, giving gain dips for the phases with largest small-signal gain and thus saturation. The phase-transfer curve then has an even larger tilt, indicating low efficiency.
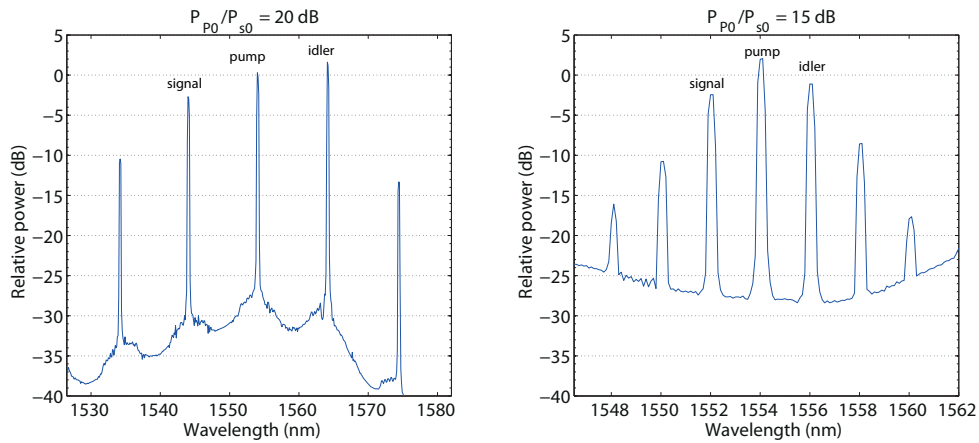

Fig. 8. PSA output optical spectra with the signal in the exponential gain regime (a) and quadratic gain regime (b).

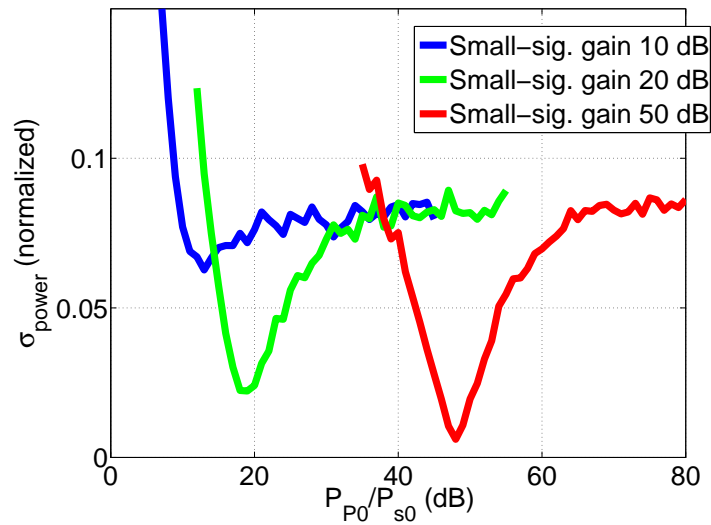However, the agreement with the three-wave model (Fig. 2(b)) is not as good here as in the

Fig. 9. Output power standard deviation vs. average input pump-to-signal power ratio. The input signal had no amplitude noise, only Gaussian phase noise with a standard deviation of 0.25 rad.

exponential-gain case. We attribute this mainly to the larger higher-order FWM in this case, as seen in the PSA output optical spectrum (Fig. 8). For the quadratic-gain case, the first higher-order FWM tones are less than 10 dB below signal and idler, respectively. In the exponential-gain case, there is instead a power assymmetry of several dB between signal and idler at the output, which we mainly attribute to the Raman-induced power transfer from signal to pump and idler, and from pump to idler. The first higher-order FWM tone on the signal side is thus only 8 dB below the the signal at the output, but well over 10 dB below the idler. The higher-order FWM tone on the idler side is even lower. The power assymmetry does not seem to significantly impair the performance, likely since the FWM is still much larger than the Raman effect.

4.   Simultaneous reduction of amplitude- and phase noise

To achieve a better understanding of which input signal power that gives the largest suppression of the PN-to-AN conversion, we investigate a binary phase-shift keyed signal (BPSK) using the three-wave model. Due to the introduced additional degradation from the SBS-suppression phase-modulation, we were not able to satisfactory measure the standard deviations experimentally. We begin with an unrealistic signal impaired only by PN, in order to study the suppression of the PN-to-AN conversion. Figure 9 shows the obtained output power standard deviation versus input average signal power from an ideally phase-matched PSA at three different pump powers giving maximal small-signal gains of 50, 20 and 10 dB, respectively. The output amplitude was normalized to one. At each average input signal power, 2000 samples was used to compute the standard deviation. The input signal and idler phase had a Gaussian distribution with a standard deviation of 0.25 radians. The mean input phase was such that the mean small-signal gain was the largest possible in each case.

In the small-signal case, the output power standard deviation is about 0.08 for all small-signal gain cases, resulting from the inherent PN-to-AN conversion. Here, the conversion from PN to AN is very good in all cases, giving an output signal with essentially no PN. In the

50 dB- and 20 dB-small-signal gain cases, the PN-to-AN conversion can be very efficiently suppressed, reaching clear minima at a signal power of 48 dB and 18 dB below the pump power, respectively, which matches the transfer-functions of Fig. 1 well. When the small-signal gain is lower, this minima is much less pronounced, as can be expected from the transfer function results. 10 dB is not a sufficient small-signal gain to suppress the PN-to-AN conversion. Of course, the power standard deviation increases significantly in all cases as the amplifier is deeply saturated.
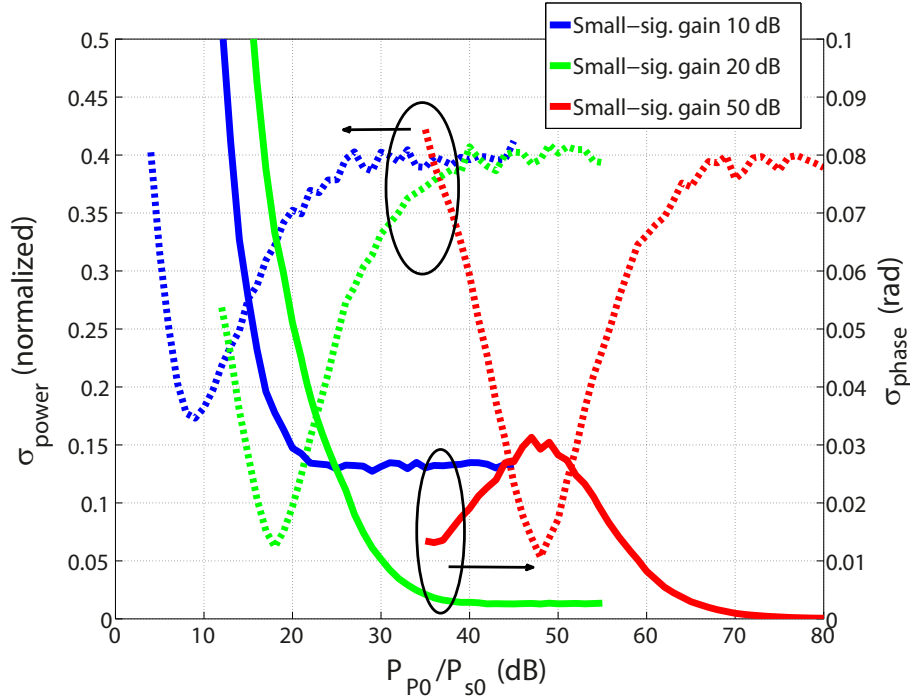

Fig. 10. Output power (solid lines) and phase (dashed lines) standard deviations vs. average input pump-to-signal power ratio. The input signal was degraded with Gaussian phase and amplitude noise with a phase standard deviation of 0.25 rad and a normalized amplitude standard deviation of 0.4.

Next, we consider signals with both phase- and amplitude noise prior to the PSA. It is well known that a phase insensitive parametric amplifier in saturation can regenerate the amplitude of a PSK signal though typically at the expense of some additional phase noise [12]. Conversely, we know that PN will be converted to AN in an unsaturated PSA. However, a real signal is likely to suffer from both AN and PN prior to regeneration, so to what extent can both be improved? To answer this question, we start with an input signal and idler whose amplitudes had a Gaussian distribution with a standard deviation of 0.4 (normalized amplitude = 1). The phase was distributed as in the PN-only case above. The obtained output phase- and amplitude standard deviations versus input average signal power are shown in Fig. 10, again for an ideally phase-matched PSA at three different pump powers giving maximal small-signal gains of 50, 20 and 10 dB, respectively. The power standard deviations vary with input pump-to-signal power ratio in a very similar way as in Fig. 9. In the small-signal regime, there is no improvement, but also no degradation of the power standard deviation, compared with the input, while the phase improvement remains very good, with a very large reduction from the original standard
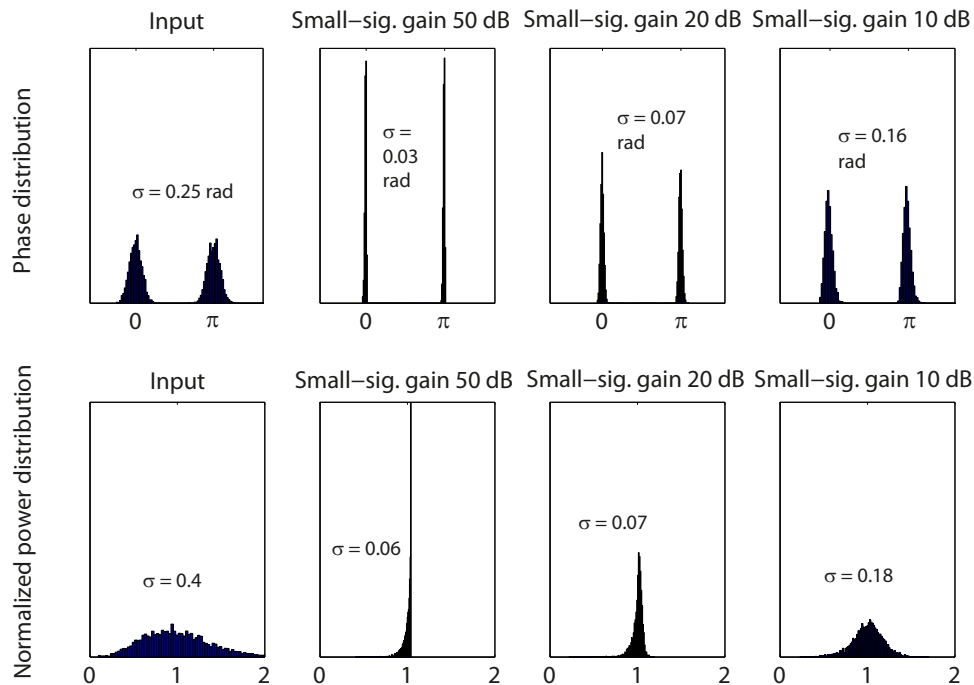
Fig. 11. Phase histograms (top row) and power histograms (bottom row) at the PSA input and output when the small-signal gain is 50, 20 and 10 dB, and the input signal power is 48, 18 and 10 dB below the pump power, respectively. The standard deviation σ is indicated in each case.

deviation of 0.25 rad for all three cases. In the 50 dB-small-signal gain case, the power standard deviation can be reduced from 0.4 down to a minimum of about 0.06 as the signal power is increased. Simultaneously, the reduction of PN, which is essentially perfect in the small-signal case, is compromised, and the phase standard deviation reaches a maximum of about 0.03 rad when the amplitude standard deviation is at its minima (input signal power 48 dB below the pump). It should be pointed out that 0.03 rad is still a large reduction from the original 0.25 rad, giving a case where both phase- and power standard deviations are reduced by nearly one order of magnitude simultaneously. For the cases of lower small-signal PSA gain, the phase standard deviation increases further when the signal power is increased; nevertheless, a reduction in both phase and power standard deviation can be achieved. Figure 11 shows phase and power histograms of the PSA output signal at the input signal power giving the lowest power standard deviation in the three different small-signal gain cases (signal power 48, 18 and 10 dB below pump power, respectively). Finally, Fig. 12 shows the signal constellation before and after the PSA. It can be observed that the clouds are significantly compressed in both amplitude and phase in the higher-gain cases, and that the output constellation assumes a somewhat "hook-like" shape, similar to the phase-trajectories shown in Fig. 1.

Note that this analysis only considers the parametric process itself and does not account for noise introduced by the PSA (amplified quantum noise, pump-transfer noise and Raman-induced noise [16]). Moreover, small frequency spacing between the interacting waves increases higher-order FWM which is not accounted for in the three-wave model. There can be many additional waves generated [17], which may limit the efficiency of the primary process
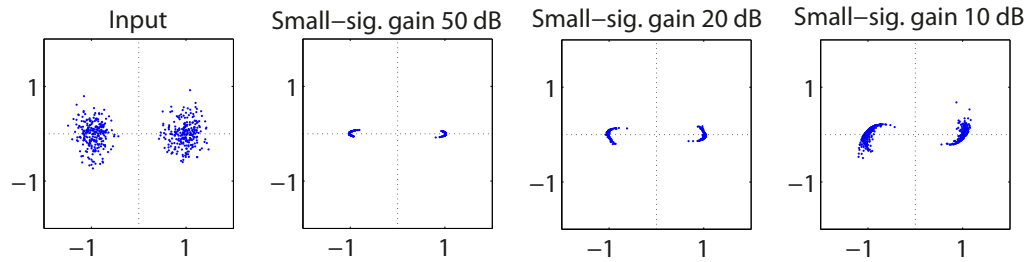
Fig. 12. Signal constellations at the PSA input and output when the small-signal gain is 50, 20 and 10 dB and the input signal power is 48, 18 and 10 dB below the pump power, respectively.

substantially. This may degrade regeneration performance further.

5. Conclusion

We have solved the three-wave model equations for a non-degenerate idler PSA operating in saturation and found that a PSA with suffient small-signal gain (e.g. 20 dB) can achieve flat phase-to-amplitude transfer functions over a wide range of phases ($> \pm 1$ rad around the center phase) while keeping the corresponding degradation of the phase-to-phase transfer function moderate ($< \pm 0.8$ rad output variation for π rad input variation). Larger PSA small-signal gains reduces this degradation further. We also confirmed that these transfer functions are achievable experimentally, with a good match between experimental results and the three-wave model. However, when there is large higher-order FWM, e.g. for small frequency-separation between signal/idler and pump, the three-wave model is no longer valid, and we found that experimental results deviated from those found numerically. A full solution of the nonlinear Schrödinger equation is then necessary to describe the system.

An optimal level of saturation giving the flattest possible phase-to-amplitude response was found to exist, and depend on the small-signal gain. For a 20 dB-gain PSA this was experimentally found to be about 22 dB pump-to-signal power ratio at the input.

Using the three-wave model, we also investigated the regenerative effect a PSA in saturation has on a signal impaired by phase and amplitude noise and found that a substantial improvement in amplitude and phase standard deviation simultaneously is possible. A PSA with a 20 dB small-signal gain can reduce the phase standard deviation by nearly a factor of four while at the same time reduce the amplitude standard deviation by more than a factor of four. If the PSA small-signal gain is larger, the regenerative effect is also larger. Moreover, since the PSA reponse can be relatively flat over a large input range in both amplitude and phase, there is good possibility to improve also the tails of the distributions.

A good PSA-based regenerator should thus be designed with sufficiently large small-signal gain. The trade-off between phase- and amplitude regeneration needs to be carefully balanced for the application, and the three-wave model can be a sufficient tool to do so in many cases.